Geomechanics and Engineering, *Vol. 39, No. 3 (2024) 283-303*
https://doi.org/10.12989/gae.2024.39.3.283

Dynamic-tracking investigation and evaluation method for rock mass engineering characteristics of adverse geologic phenomena during construction

Yihan Du[1,2,3], Wei Han*[1,3], Dexin Nie[2], Yufeng Wei[2] and Mo Zhang[2]

[1]*School of Architecture and Civil Engineering, Anhui Polytechnic University, Wuhu 241000, China*
[2]*College of Environment and Civil Engineering, Chengdu University of Technology, Chengdu 610059, China*
[3]*Engineering Research Center of Anhui Green Building and Digital Construction, Anhui Polytechnic University, Wuhu 241000, China*

(*Received May 6, 2021, Revised September 28, 2024, Accepted October 13, 2024*)

Abstract. In large-scale engineering construction, there are many cases of highly concealed adverse geological phenomena (HCAGP) at certain scale that are not revealed until excavation. It is crucial to ascertain their geological characteristics and rapidly formulate treatment since they often have enormous negative impacts on the project. However, conventional exploration and evaluation methods are not suitable for HCAGP due to the long acquisition time and strict requirements. Therefore, this paper proposes a dynamic-tracking investigation and evaluation method (DTIEM), which carries out a series of fast and effective techniques, including down-the-hole (DTH) drilling, cross-inclined holes, seismic tomography and P-wave velocity (V_P) tests, for preliminary data of HCAGP. Then, an initial treatment plan is proposed to guide the construction. Subsequently, the initial data of the HCAGP are tracked and revised until the end of construction. This method was applied to a deep groove at a hydropower station, which was exposed when the excavation of dam section 11. The results show that by using the DTIEM, the preliminary engineering characteristics of the deep groove were obtained quickly. The rock mass quality of the top deep groove was grade III_2 with 9.82 GPa, the middle part was grade III_1 with 15.07 GPa, and the bottom part was grade II with 19.68 GPa. The quality of rock mass gradually increases with the increase of depth. From the numerical simulation, the maximum additional displacement is about 20 mm at the dam crest, 4 ~ 7 mm at the dam heel, and 2 ~ 5 mm at the dam toe. The numerical simulation and monitoring results show that the stress and strain of the dam and foundation are within a safe range in each stage. Thus, the proposed method is feasible.

Keywords: down-the-hole (DTH); dynamic-tracking investigation and evaluation method (DTIEM); highly concealed adverse geological phenomena (HCAGP); P-wave velocity

1. Introduction

Currently, advanced geological prediction disaster prevention and control is widely used in tunnel engineering for unfavourable geological conditions. Advanced geological prediction mainly adopts advanced drilling, geophysical prospecting, and other methods to determine further the engineering geological and hydrogeological conditions in front of tunnel excavation, which guides the smooth progress of engineering construction and reduce the probability and degree of harm caused by geological disasters. Different from the linear construction trajectory of tunnel engineering, in hydropower station engineering, dam foundation excavation mainly depends on the preliminary investigation results. However, the initial investigation is still unable to reveal all the adverse geologic phenomena in dam foundations. We define it as highly concealed adverse geological phenomena (HCAGP) that cannot be revealed until excavation and considerably influences the project, which usually leads to doubt about the feasibility of the project, prolonging the construction period. Especially in hydropower projects, dam foundations under modern riverbed sections are always the most difficult areas for exploration with the most complicated geological conditions, in which HCAGP may be hidden. If not properly handled, HCAGP may cause large losses. For example, during the construction of the Bapanxia Hydropower Station, the axis of the dam moved 104 m upstream due to geological problems of the dam foundation (Liu 2016). After the dam foundation excavation of the Xiangjiaba hydropower station, a compressive zone and a flexural crushed zone were discovered (Yu 2007). Then, large-scale groove excavation and replacement were carried out. The construction period was extended greatly. Hence, it is of great practical significance to evaluate the engineering characteristics of HCAGP rapidly and accurately to minimize the influence on the project.

Usually, in the investigation stage of hydropower project, conventional investigation methods can be used to investigate and evaluate (Bednarek *et al.* 2020, Kim *et al.* 2022, Kim *et al.* 2019), including engineering geological mapping, geophysical prospecting, boreholes, adits, inclined wells, geophysical exploration and in-hole imaging

*Corresponding author, Ph.D.
E-mail: han1017@mail.ahpu.edu.cn

ISSN: 2005-307X (Print), 2092-6219 (Online)

Table 1 Unloading index of rock mass in dam foundation of Xiluodu, Xiaowan, and Laxiwa hydropower station

Hydropower station	Unloading zone	V_P (m/s)	Joint opening (cm)	Lithology
Xiluodu hydropower station	Strongly unloading zone	< 2500	> 2	Basalt
	Weakly unloading zone	> 4800	0 ~ 2	
	Undisturbed zone	> 4800	0	
Xiaowan hydropower station	Strongly unloading zone	< 2500	> 2	Gneiss
	Weakly unloading	3000 ~ 4000	0.2 ~ 2	
Laxiwa hydropower station	Strongly unloading zone	< 2500	> 1	Granite
	Weakly unloading zone	< 4100	0.1 ~ 1	

technology (Alemdag *et al.* 2015, Cai *et al.* 2004). Nevertheless, drilling takes a long time with a large working platform, and the results of geophysical exploration methods could be more accurate. Therefore, these methods cannot be adopted for HCAGP due to the shortage of time, narrow working platform and high requirement for investigation precision during the construction phase.

Therefore, this paper proposes a dynamic-tracking investigation and evaluation method to quickly identify the adverse geological phenomena exposed by dam foundation excavation. Once the HCAGP under a foundation is exposed, an investigation is carried out with efficient investigation techniques and rapid evaluation methods (Palmstrom *et al.* 2001, Kayabasi *et al.* 2003), and preliminary investigation results are obtained. Subsequently, the treatment is formulated to guide the initial construction. Continuously track, feed back and optimize data during the construction process until the end of the construction. Finally, the optimal data of rock mass engineering characteristics with HCAGP are obtained. The method minimizes the working cycle and ensures the accuracy of evaluation.

2. Dynamic-tracking investigation and evaluation method (DTIEM)

2.1 Investigating method

Drilling, pit exploration and in situ testing generally require mechanical and power equipment, which consume human resources, material resources. Therefore, more than these methods are needed for rapid, special investigation and evaluation of HCAGP.

Down-the-hole (DTH) drilling is usually used for anchor cable holes, bolt holes, blasting holes and grouting holes in engineering, with drilling diameters from 80 mm to 120 mm. The DTH machine is portable and easy to move, has high mechanical efficiency and work efficiency, and is relatively low cost. It can effectively overcome the main obstacles of narrow operating platforms and urgent time limits. Moreover, the P-wave test can be carried out using DTH. Therefore, adits, vertical shafts and inclined shafts can be optimized for horizontal, vertical and oblique DTH evaluations.

Common geophysical prospecting methods include the ground electrical sounding method (Feng *et al*. 2009), overwater electric sounding method, shallow seismic reflection method, high-density resistivity method, geological radar method, controlled source audio-frequency magnetotelluric (CSAMT) (Chen *et al.* 2015), and etc. The electric sounding method is unable to detect the spatial distribution of the transition rock interface accurately. The overburden has a great influence on the detection results of the high-density resistivity method. The frequency of the selected antenna will affect the detection results of the geological radar method. In the shallow seismic reflection wave method, the detection results are often affected by improper parameter selection. When the dielectric electrical structure in CSAMT is complex, the analytical solution cannot be obtained, and the inversion problem is more complicated. In other words, geophysical data have multiple solutions, so the spatial distribution and engineering characteristics of adverse geological phenomena cannot be accurately ascertained by using only the geophysical exploration method.

2.2. Evaluation method

Conventional engineering evaluation of rock mass characteristic is mainly based on structural plane spacing (D), integrity coefficient (K_V) (Yin *et al.* 2021), rock quality designation (RQD) (Yin *et al.* 2021, Jiang *et al.* 2009; Hasan *et al.* 2023), joint number per cubic meter (Jv), strength parameters, and deformation parameters (Que *et al.* 2023). These parameters cannot be easily obtained in the investigation of HCAGP, so a more convenient evaluation system should be established (Aydan *et al.* 2014).

P-wave test is used to judge the integrity of the rock mass based on the difference in propagation velocity and absorption of elastic waves in different elastic media (Song *et al.* 2014). In hard rock with uniform lithology, the P-wave propagation velocity is faster to Conversely, in rock mass containing structural planes, structural planes will significantly reduce the acoustic wave velocity. Some hard rocks will release stored high elastic strain energy and form more structural planes once subjected to strong tectonic action. Nevertheless, if in situ and not disturbed, the rock mass is still in a compact mosaic state. Even if the structural plane spacing is small, the rock mass still has high strength and low permeability, that is, similar integrity in mechanical

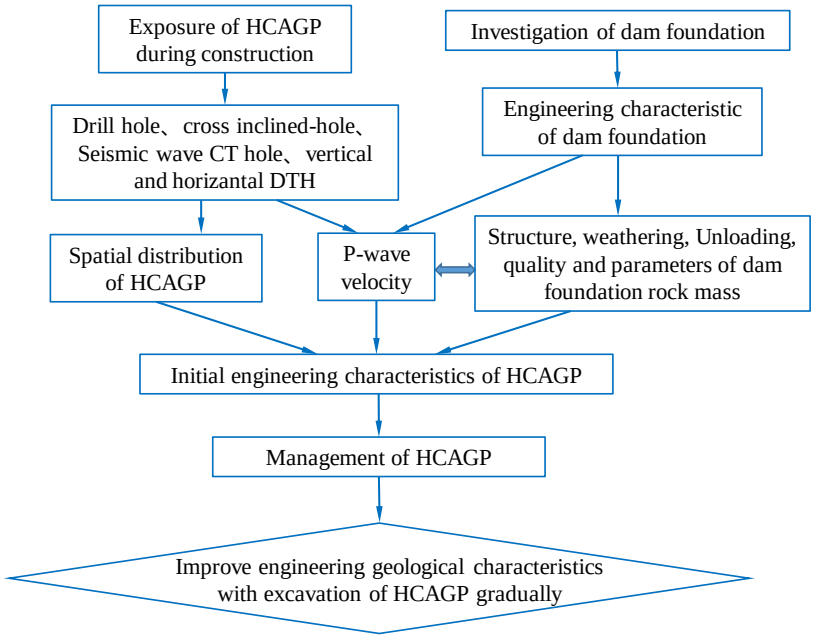

Fig. 1 Flow chart of dynamic-tracking investigation and evaluation method

properties with high P-wave velocity. Therefore, some indexes such as structural plane spacing cannot truly reflect mechanical properties, especially deep in situ rock masses. In contrast, P-wave velocity (V_P) can more objectively reflect the real mechanical properties.

In China, V_P has been used as a conventional indicator for rock mass detection and evaluation of dam foundation, such as for the Xiluodu hydropower station, Baihetan hydropower station, Guanyinyan hydropower station, Xiangjiaba hydropower station, Laxiwa hydropower station, and Longkaikou hydropower station (Lu *et al*. 1996, Zhang 2010). For example, Table 1 shows the statistics of some large hydropower projects in China which divide unloading zones according to V_P.

Rock mass structure is an index to evaluate the integrity of rock masses through the development and distribution of structural planes. It is found that the more developed the structural planes are, the looser the rock mass. However, in deep parts, even with developed fracture zones, the rock mass is in a state of tight mosaic structure with high strength. The structural plane interval only shows the size of the rock cut by structural plane. V_P reflects the engineering mechanical properties precisely, which is more representative of evaluating the real rock mass. Therefore, we can divide the rock mass structure by V_P. Rock weathering is a comprehensive change in the original structural and engineering characteristics of exposed or near-surface rock masses under the action of external dynamic geology, including the rock's physical state, mineral composition and structural planes, which will lead to the deterioration of integrity and the reduction in mechanical parameters. The classification of weathering zones is mainly based on the RQD value, coring rate, permeability, strength characteristics, wave velocity ratio and integrity coefficient. The unloading zone of a valley slope is caused by valley erosion, which leads to stress redistribution. The rock mass on the surface of a valley slope bounces back toward the free face, resulting in a decrease in the rock mass stress, further development of original cracks, and the formation of new unloading cracks. Unloading tensile cracks lead to a very low wave velocity. Therefore, fracture development is the manifestation of the unloading zone. The V_P can characterize fracture development and judge the degree of unloading well.

It can be speculated that a good-quality rock mass has higher mechanical properties with higher V_P. In addition, the P-wave test is more convenient and rapid, which can be implemented through DTH methods. Therefore, V_P is mainly used in the DTIEM of the rock mass for HCAGP. Furthermore, horizontally compared, HCAGP is attached to the normal rock mass of the foundation and bound to have an internal connection with it. Therefore, the research results of normal rock masses in other dam sections can be used to evaluate adverse geological phenomena.

Accordingly, the DTIEM for an adverse geological rock mass is as follows:

Investigate the geometry and rock mass once HCAGP is exposed. First, a small number of vertical boreholes are arranged along the longitudinal axis to determine the trend of the changes at depth. Then, a large number of vertical drill holes and a small number of cross-inclined holes are arranged on both sides to roughly control its boundary. Make sure that each pair of cross-inclined holes is oriented to achieve the objectives.

After the boundary is roughly identified, pairs of vertical holes are drilled on both sides of the HCAGP for cross-hole seismic tomography to obtain an accurate boundary of each transverse section. Then, the boundary data are modified, and an optimized 3D image of the HCAGP is obtained.

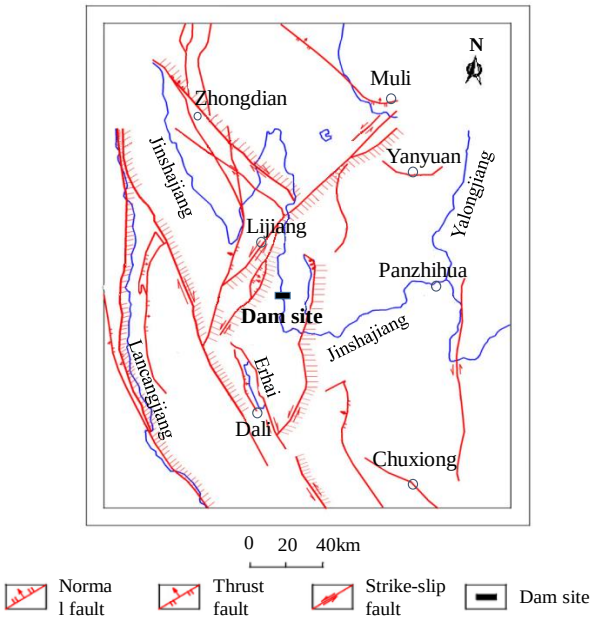

Fig. 2 Geographic location and general structure of the hydropower station

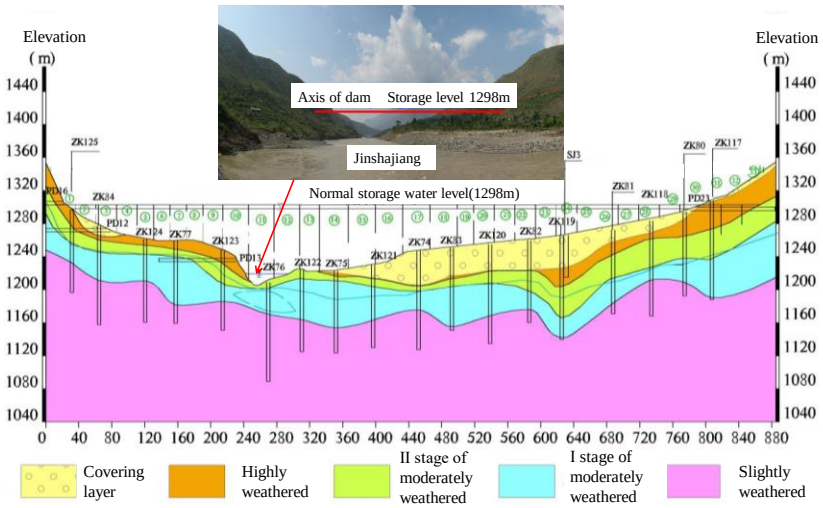

Fig. 3 Engineering geological profile of dam axis and photo of bedrock at the dam axis

According to the data on rock mass engineering characteristics at the investigation stage, the correlations between the normal rock mass and the V_P could be analyzed. To obtain the correlation between the V_P and HCAGP, the P-wave tests are conducted in all boreholes, and DTH drillings are used to analyze the variation in V_P in different directions. Determine the rock mass structure by the V_P (Pappalardo 2015), the weathering zone by the wave velocity ratio, the unloading zone by the P-wave gap, and the rock mass quality by the V_P and wave velocity ratio. Mechanical parameters are obtained by V_P as well (Kahraman and Yeken 2008, Sarkar *et al.* 2012). Combined with the optimized 3D images, form the initial data of the HCAGP for treatment scheme and construction.

Continuously detail three-dimensional boundary and engineering characteristics by tracking rock mass excavation step by step. Before completion, set devices at crucial locations to monitor deformation during construction and operation.

This set of special evaluation methods almost synchronously completes the evaluation and excavation of HCAGP. It not only has a certain accuracy but also saves time to the greatest extent. The flow chart is shown in Fig. 1.

3. Case study

3.1 Study area

A hydropower station is located in Dali, Yunnan Province, with an installed capacity of 1800 MW and a maximum dam height of 116 m. The lithology of the dam foundation is basalt. No regional faults pass through the study area (Fig. 2), and bedrock outcrops on both sides of the riverbed (Fig. 3). According to the code requirements, the minimum interval of boreholes along the dam axis

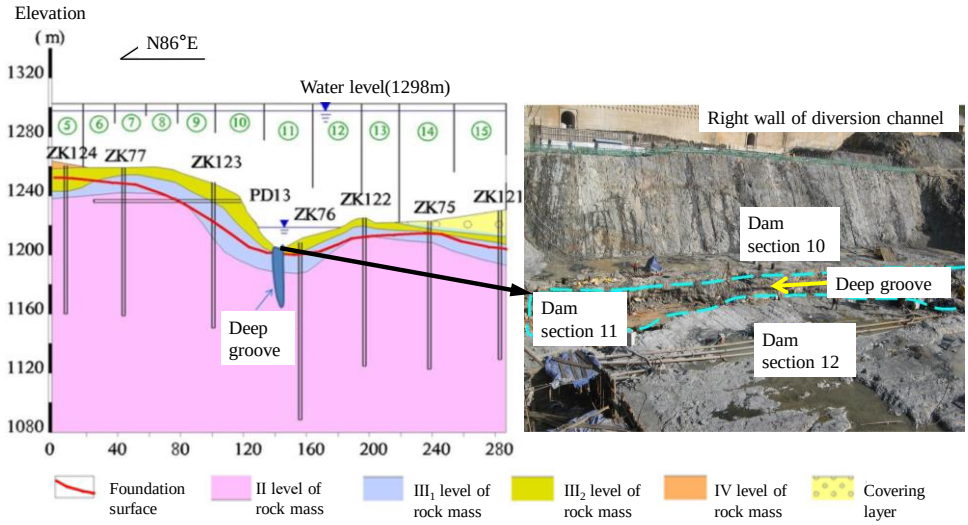

Fig. 4 The section of the dam axis and photo of the deep groove exposed during the construction of the dam section 11

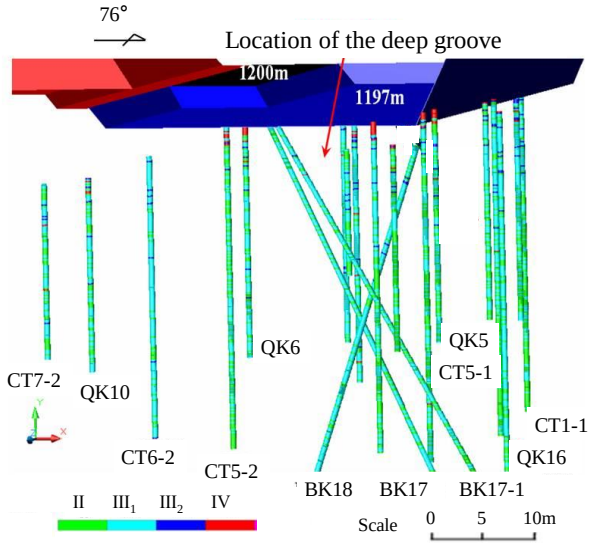

Fig. 5 Layout plan of vertical DTH, cross inclined-hole and seismic tomography cross-hole

during the exploration stage is 30 m. Borehole ZK76, which was drilled in the riverbed, did not reveal any adverse geological phenomena. After several years of investigation and demonstration, the engineering geological profile of the dam axis was obtained as shown in Fig. 3. It can be seen from the figure that the thickest overburden layer at the axis of the dam was about 40 meters. The rock masses below the elevation of 1120 m were all moderately or slightly weathered rock masses. The rock masses were relatively complete and had high strength. There were no large faults in the dam foundation. The rock mass at the riverbed position was stage II of moderately weathered rock mass, so it was speculated that the rock mass quality of the riverbed was good.

Construction of the project started at the end of 2007. Most of the dam sections had been completed by October 2010. However, when the foundation of overflow dam section 11, where the riverbed was located, was excavated to an elevation of 1197 m, a deep groove with a depth of approximately 40 m and a minimum width of only 6 m was exposed for the first time (Fig. 4). The groove was covered by a considerable amount of sand and gravel, which had a substantial adverse impact on the project. However, due to the narrow working platform, tens of meters of coverage, and time limits, it was difficult to obtain the spatial morphology and engineering geological characteristics of the deep groove accurately and rapidly using traditional investigation methods. Therefore, the DTIEM was used in the deep groove.

3.2 Exploration technology and spatial geometry of the deep groove

According to the DTIEM, nine vertical boreholes were first arranged longitudinally to penetrate the covering layer and determine the change in depth. Vertical DTH and cross-inclined holes (BK17, Bk17-1, and BK18) were placed on both sides to control the approximate boundary of the deep

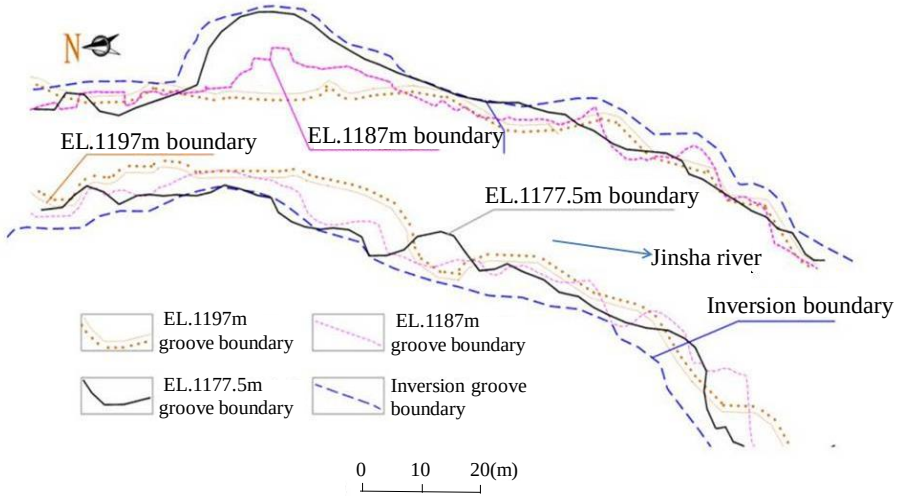

Fig. 6 Overlay chart of deep groove boundary line at different elevation

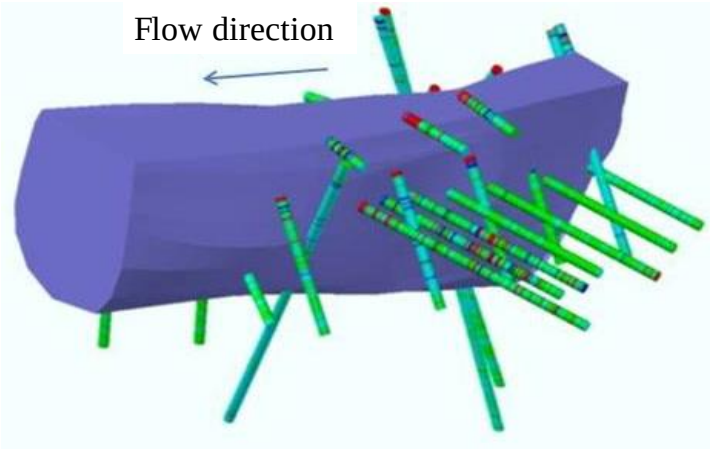

Fig. 7 The optimal 3D image of the deep groove boundary in the dam foundation region

groove (Fig. 5). Seven pairs of seismic tomography cross-holes were placed along both sides of the deep groove to form seven detection transverse profiles with intervals of 13~20 m each. The holes were all designed to be 49 m in depth, deeper than the deepest depth measured by vertical drilling.

According to the boundary data from the vertical DTH, cross-inclined holes and seismic tomography cross-hole, the initial 3D image of the deep groove was generated. By continuously modifying the deep groove boundary according to the revealed boundary of different elevations (Fig. 6) until the end of the excavation, the optimal 3D image was obtained, as shown in Fig. 7.

4. Weathering relaxation and rock mass structure

Through tracking evaluation in different stages, the engineering characteristics of the deep groove rock mass were gradually obtained. In the exploration stage, the hidden deep groove reflected its high concealment. In the early disclosure stage, a large number of exploration methods were arranged to preliminarily study the deep groove. In the middle excavation stage, exploration was further intensified, and the spatial form and rock mass evaluation of the deep groove was continuously refined. At the end of the excavation, the availability of the deep groove rock mass was evaluated to provide important data support for further design and construction.

4.1 Rock mass structure

According to the division of the rock mass structure of dam foundation at this hydropower station, the relationship between the rock mass structure and V_P is as follows: fractured structure with V_P less than 3100 m/s, mosaic structure with V_P of 3100 m/s ~ 4000 m/s, compact mosaic structure with V_P of 4000 m/s ~ 4800 m/s, submassive structure with V_P of 4800 m/s ~ 5500 m/s, and blocky structure with V_P of more than 5500 m/s.

A sketch diagram of the exposed rock mass at an elevation of 1197 m on both sides of the deep groove is shown in Fig. 8. The rock mass structure features are

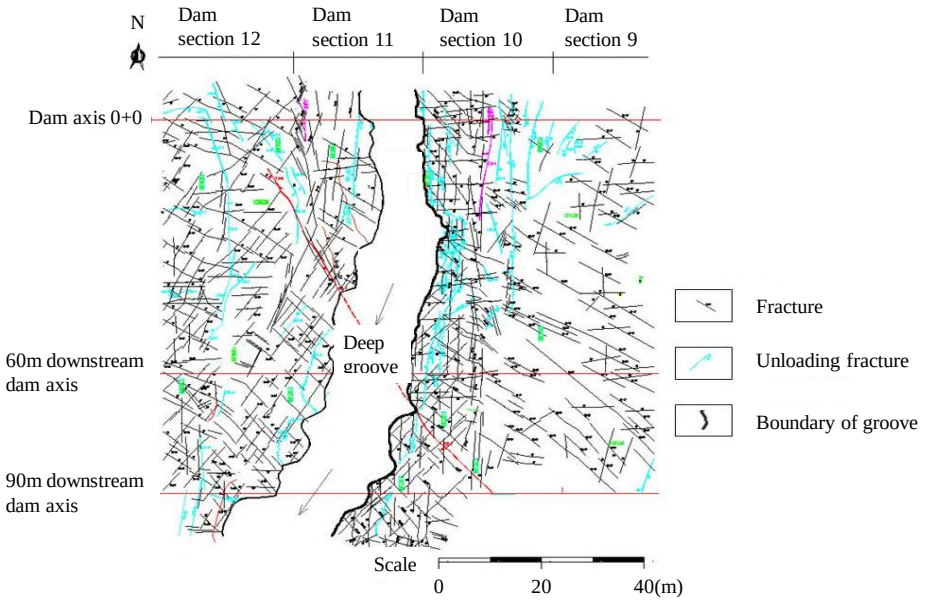

Fig. 8 The sketch diagram of the exposed rock mass structure at the height of 1197 m on both sides of the deep groove

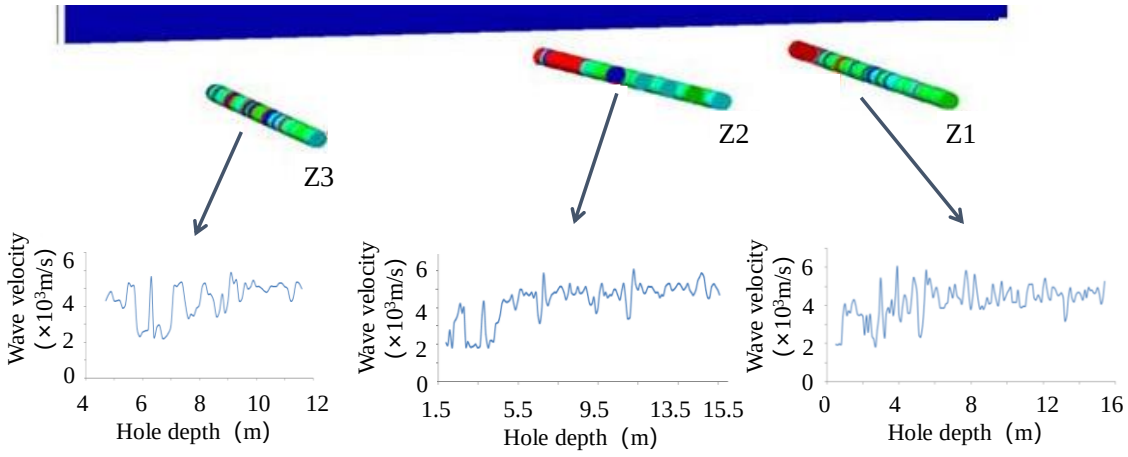

(a) Z3 (b) Z2 (c) Z1

Fig. 9 Spatial position of Z1, Z2 and Z3 in left groove wall at elevation of 1195 m and curve of P-wave velocity

similar to those of the normal rock mass. Therefore, the rock mass structure of the deep groove can be divided by the standard of the normal rock mass in other dam sections.

The V_P-depth curves of horizontal DTH Z1, Z2 and Z3 at elevations of 1195 m on the left side of the deep groove are shown in Fig. 9.

As seen from Fig. 9, taking the surface of the groove wall as 0, the V_P of rock mass within the depth range of 0 ~ 5 m is relatively low, mainly 2000 m/s ~ 4000 m/s. With the increase of hole depth, the wave velocity increases to 4000 m/s ~ 6000 m/s, which is consistent with the statistical results of the structural plane on both sides of the deep groove (Fig. 8). The rock mass structure is mainly composed of mosaic structures in the area. The unloading cracks are parallel to the strike of the deep groove. With increasing hole depth, the rock mass structure plane decreases significantly, especially unloading cracks, and the rock mass structure gradually improves to a submassive structure.

According to the P-wave test results of vertical drilling, vertical DTH, cross-inclined hole, CT hole, horizontal DTH, and the development regularity of the exposed surface structure, the transformation of the rock mass structure was speculated, and the initial rock mass structural data of the deep groove was formed.

As the deep groove wall was gradually exposed, detailed statistics of the structural plane were obtained, as shown in Fig. 10. Inclined holes were drilled in the exposed rock mass layer by layer for P-wave tests (Fig. 11) to check the suitability of the classification standard, and constantly refine the rock mass structure of the deep groove. The tests continuously "revealed, rechecked and predicted"

Table 2 Classification standard of rock weathering zone in dam foundation

Zone of weathering		Wave velocity indicators				
		K_B	Kv	Modified Kv	Modified K_B	Modified V_P (m/s)
Completely weathered		< 0.40	< 0.16	< 0.15	< 0.39	< 2500
Highly weathered		0.40 ~ 0.60	0.16 ~ 0.36	0.15 ~ 0.35	0.39 ~ 0.6	2500 ~ 3800
Moderately weathered	II	0.60 ~ 0.70	0.49 ~ 0.64	0.35 ~ 0.45	0.6 ~ 0.67	3800 ~ 4400
	I	0.70 ~ 0.80	0.49 ~ 0.64	0.45~0.64	0.67 ~ 0.80	4400 ~ 5000
S Slightly weathered		> 0.80	> 0.64	>0.64	> 0.80	> 5000

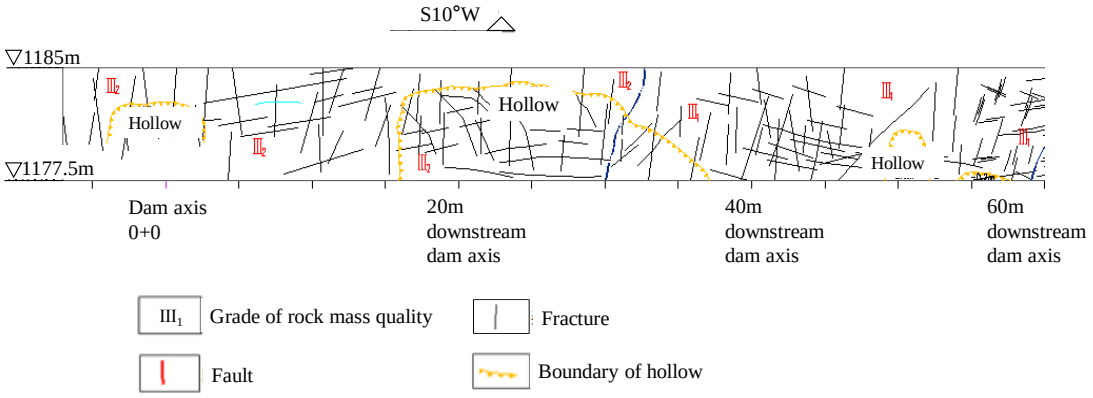

Fig. 10 Developed sketch of structural surface on left groove wall with elevation from 1177.5 to 1185 m

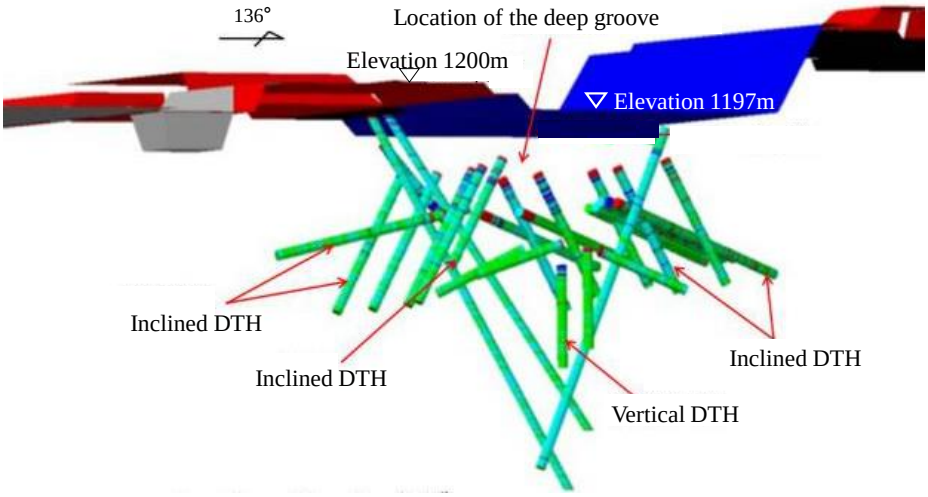

Fig. 11 Spatial distribution of inclined DTH and cross inclined-hole

conditions until the bottom of the groove. Based on the results above, the optimal rock mass structural data of the deep grooves were formed, which provided the research basis for the suitability of the deep groove rock mass.

The results of the deep groove excavation showed that structural planes were more developed closer to the upper part. The closer to the bottom, the better the rock mass was. The upper part of the groove wall was mainly composed of mosaic structure, the middle part of mosaic ~ submassive structure, and the bottom part of submassive ~ massive structure (Fig. 12), which was consistent with the preliminary rock mass structural data of the groove.

4.2 Zone of weathering

The quantitative classification of weathering zones at this hydropower station (Table 2) was obtained by slightly modifying the integrity coefficient of the national standard, the characteristics of weathering zones and a large number of tests on the dam foundation. The weathering conditions and characteristics of the deep groove rock mass were basically consistent with the dam foundation. Therefore, the weathering zone classification standard of the dam foundation can be applied to the deep groove rock mass.

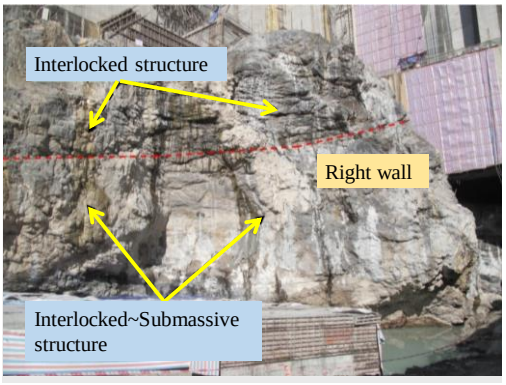

(a) Right wall

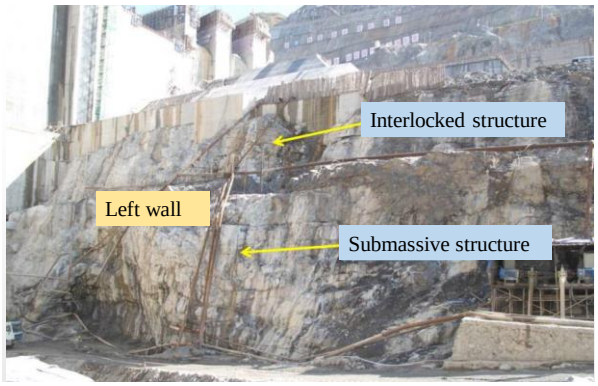

(b) Left wall

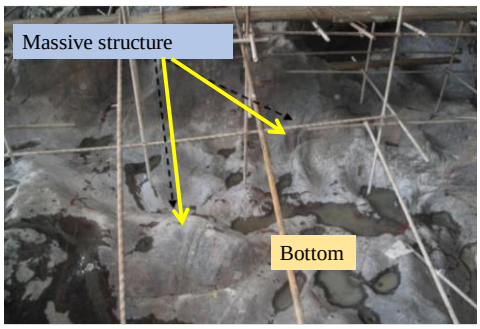

(c) Bottom

Fig. 12 Rock mass structure of left wall, right wall and bottom of deep groove

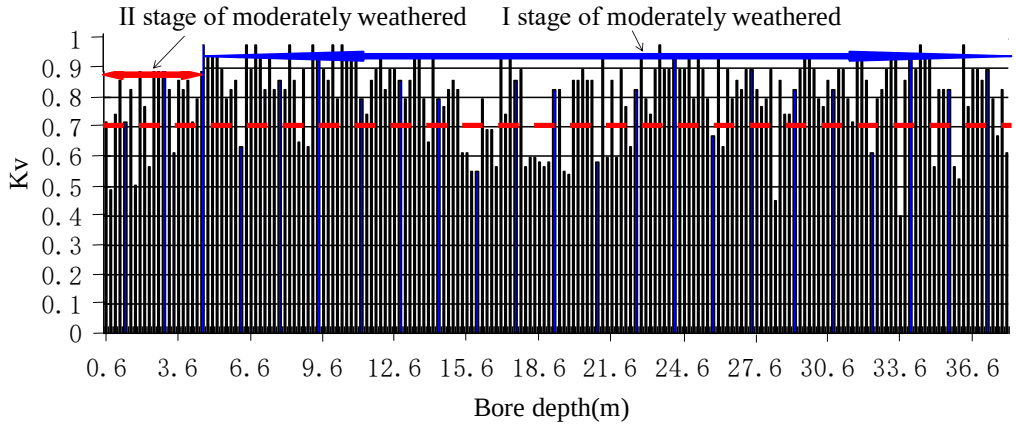

Fig. 13 Corrected Kv histogram of SC-1 on the left wall of deep groove

In the table, wave speed ratio K_B is the ratio of the measured wave velocity to the wave velocity of the intact rock. Kv equals the square of K_B named integrity coefficient. Combining with the in situ situation of the rock mass, the weathering zone of the deep groove rock mass was divided quantitatively. The wave velocity ratio of 0.60 was taken as the boundary between highly weathered and stage II of moderately weathered, 0.70 as the boundary of stage II and stage I of moderately weathered, and 0.80 as the boundary of stage I of moderately weathered and slightly weathered. The V_P ratio with hole depth of hole SC-1 is shown in Fig. 13. Within the hole depth range of 0 to 4.4 m, the wave velocity ratio is mostly lower than 0.60. In the range of 13.2 m to the bottom, the wave velocity ratio is mostly higher than 0.67 and partly higher than 0.80.

Combined with the rock mass at the opening of hole SC-1, the hole depth of 0 ~ 4.4 m is divided into stage II of the moderately weathered zone and 4.4 ~ 36 m is the stage I of the moderately weathered zone.

According to the division standard, the preliminary weathering zone data of the deep groove were deduced by the Kv of all drilling holes. It was speculated that the weathering belt of the upper part was thicker than that of the bottom part.

As the deep groove was excavated layer by layer, according to the velocity data of inclined DTH drilling at different elevations, the weathering boundary was gradually refined, as shown in Fig. 14. The weathering zone model can be cut in any position and any direction to obtain the weathering zone boundary of the groove rock mass.

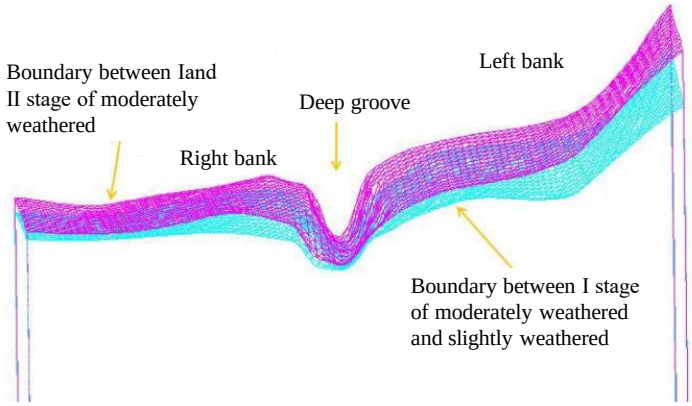

Fig. 14 Three-dimensional display of the optimal weathering zones

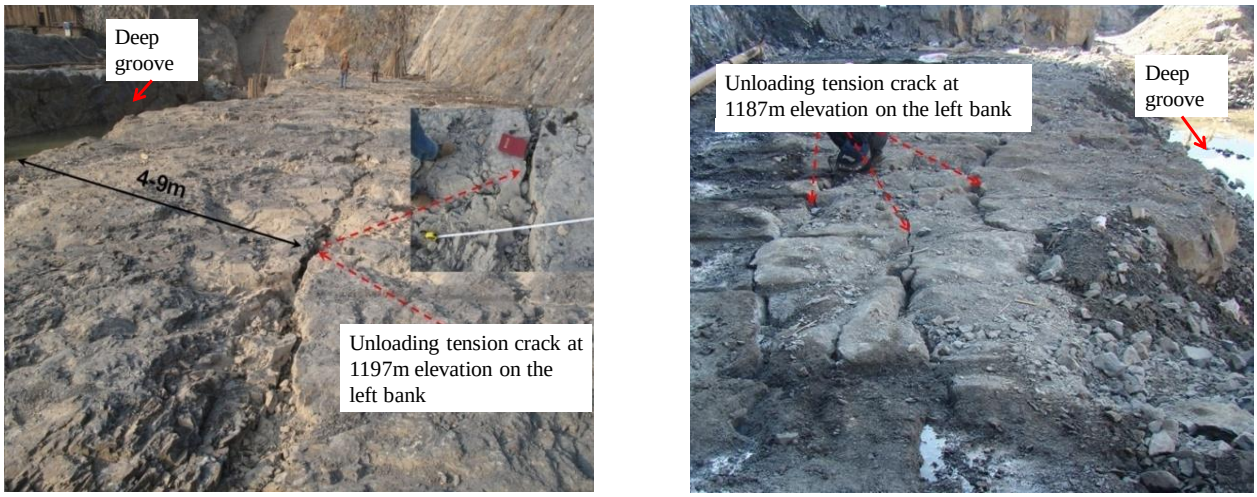

(a) Elevation of 1197 m (b) Elevation of 1187 m

Fig. 15 Photos of unloading cracks at different elevations on the left bank of deep groove: (a) Unloading fracture at elevation of 1197 m and (b) Unloading fracture at height of 1187 m

Due to the continuous erosion by water during the formation of the deep groove, the upper rock mass was first exposed and unloaded toward the surface. Under the action of weathering, the physical and mechanical properties of the original rock changed, and the integrity decreased. Therefore, the weathering zone of the upper part of the groove was the thickest. The tremendous mechanical power of the flowing water eroded the rock mass at the bottom. The weathered rock masses were carried away by erosion. Therefore, the rock mass at the bottom of the weak weathering belt was the lowest part of weathering, with the thickness of only 0.5 ~ 1 m. After the excavation, the variation in weathering of the deep groove was revealed, which was the same as that in the preliminary data.

4.3 Unloading

The unloading of the rock mass on the valley slope is caused by valley erosion, which leads to stress redistribution. The rock mass on the slope's surface bounces back toward the free face, resulting in a decrease in stress, further development of the original crack, and the formation of new unloading cracks. Fracture development is the manifestation of the unloading zone. V_P can characterize the degree of fracture development and unloading well. The unloading zone classification of dam foundation rock mass in this hydropower station also proved the correlation between V_P and the unloading zone.

Due to the evolutionary process, the unloading of the deep groove and valley slope were the same in nature but different in magnitude. Therefore, similar to the unloading of the valley slope, tension fractures nearly parallel to the free face occurred in both banks of deep groove due to the strain difference between the unloading and undisturbed zones and the existing structural tension expanded. Taking elevations of 1197 m and 1187 m (Fig. 15) on the left bank of the deep groove as examples, the direction of the unloading fracture was roughly parallel to the strike of the deep groove, with a serrated shape and a long length, which was a typical tensile fracture.

The unloading zone below the 1187 m elevation of the deep groove was divided according to the P-wave test results of DTH drilling. Each hole was tested. If there were tensile unloading cracks in one measurement section of 20 cm, the value of V_P should decrease sharply, generally 2000 ~ 3000 m/s lower than that of intact rock. If there was

Table 3 Classification of rock mass quality of the dam foundation

Rock mass grade		Main index						
		Structural type of rock mass	V_P (m/s)	K_V	q (Lu)	E_0 (GPa)	f'	c'
II		Submassive-massive structure	> 5200	> 0.68	< 0.6	> 15	> 1.2	> 1.6
III	III_1	Submassive~compact mosaic structure	4000 ~ 5200	0.4 ~ 0.68	0.6 ~ 4	8 ~ 15	1.0 ~ 1.2	1.2 ~ 1.6
	III_2	Mosaic structure	3100 ~ 4000	0.25 ~ 0.4	4 ~ 10	4 ~ 8	0.8 ~ 1.0	0.8 ~ 1.2
IV		Mosaic -cataclastic structure	2500 ~ 3100	0.15 ~ 0.25	> 10	2 ~ 4	0.55 ~ 0.8	0.5 ~ 0.8
V		Cataclastic structure	< 2500	< 0.15	> 10	< 2		

Table 4 Rock mass quality classification of DTH LSC-3

Depth (m)	V_P (m/s)	K_V	Grade	Depth (m)	V_P (m/s)	K_V	Grade	Depth (m)	V_P (m/s)	K_V	Grade
1.2	3509	0.57		10.8	5797	0.94		21.6	6061	0.98	
1.6	2721	0.44	IV	11.6	5333	0.86		22.2	6061	0.98	
2	3175	0.51		12.2	5797	0.94		23	5333	0.86	
2.2	4598	0.74		13	4444	0.72		23.8	5556	0.90	
3	5128	0.83		13.8	4938	0.80		24.6	5797	0.94	
3.8	4938	0.80		14.6	5333	0.86		25.4	3333	0.54	
4.6	5333	0.86	III_2	15.4	6061	0.98		26.2	5556	0.90	
5.4	5128	0.83		16.2	5797	0.94		27	5797	0.94	
6.2	5333	0.86		17	4040	0.65	III_1	27.6	5128	0.83	III_1
7.4	3252	0.52		18.4	5333	0.86		29.2	5556	0.90	
7.6	4938	0.80		19.2	5797	0.94		30	5333	0.86	
8.4	5333	0.86	III_1	20	5128	0.83		30.8	5128	0.83	
9.2	5797	0.94		20.8	4938	0.80		31	5333	0.86	

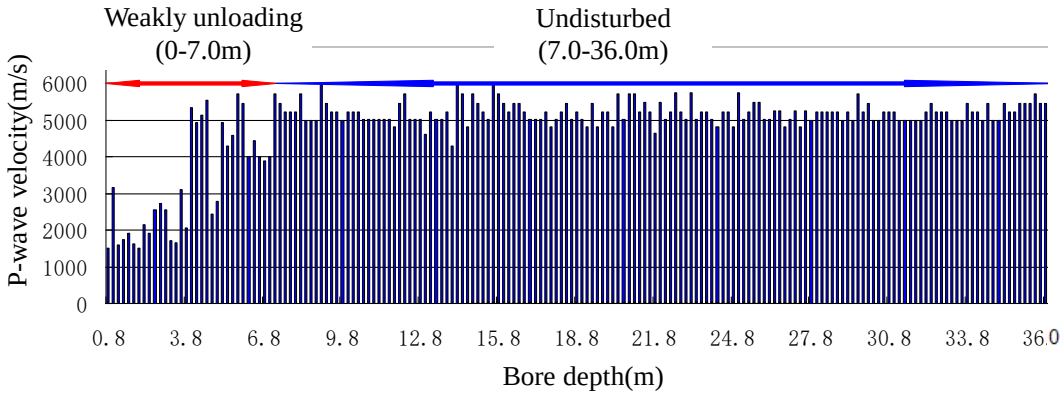

Fig. 16 Unloading zone division of P-wave velocity column diagram of DTH SC-7

no tensile fracture, the wave velocity value should be relatively high, close to that of the intact rock mass. Therefore, the wave velocity with hole depth column diagram shows a low wave velocity, where the unloading tensile crack occurs, accordingly dividing the unloading zone. The division of the unloading zone of inclined hole SC-7 on the right wall of the deep groove at 1187 m is shown in Fig. 16.

According to the unloading pattern of the valley, it is speculated that the upper part of the unloading zone is the thickest and gradually decreases to the bottom. Combined with the unloading fracture and the P-wave test, the preliminary data of the unloading zone of the deep groove were formed to guide exposition. As the deep groove was exposed, the inclined hole of the groove wall was arranged layer by layer during construction. Accordingly, the unloading data were improved step by step. Finally, the optimal data for the unloading belt was obtained. The transverse section of the 36.7 m downstream dam axis is taken as an example, as shown in Fig. 17.

The unloading depth of the deep groove on the left wall is relatively thinner than that on the right. The maximum

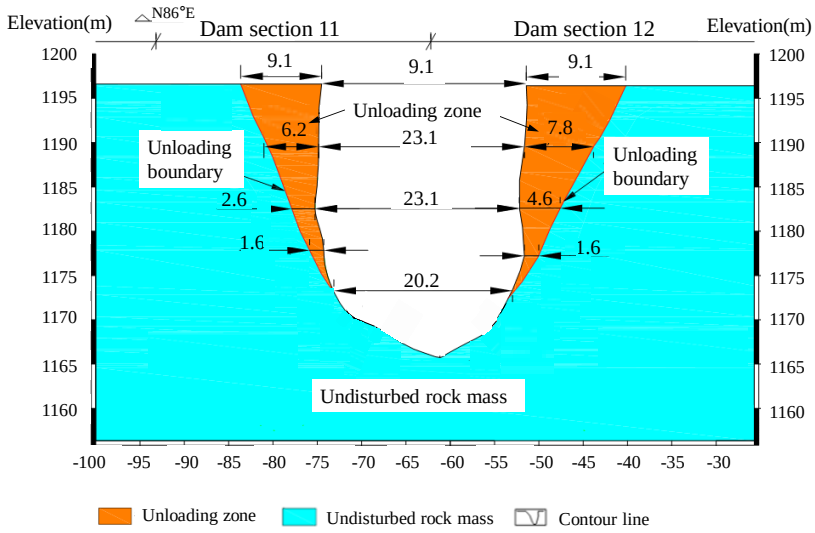

Fig. 17 Deep groove unloading zone of 36.7 m downstream dam axis section

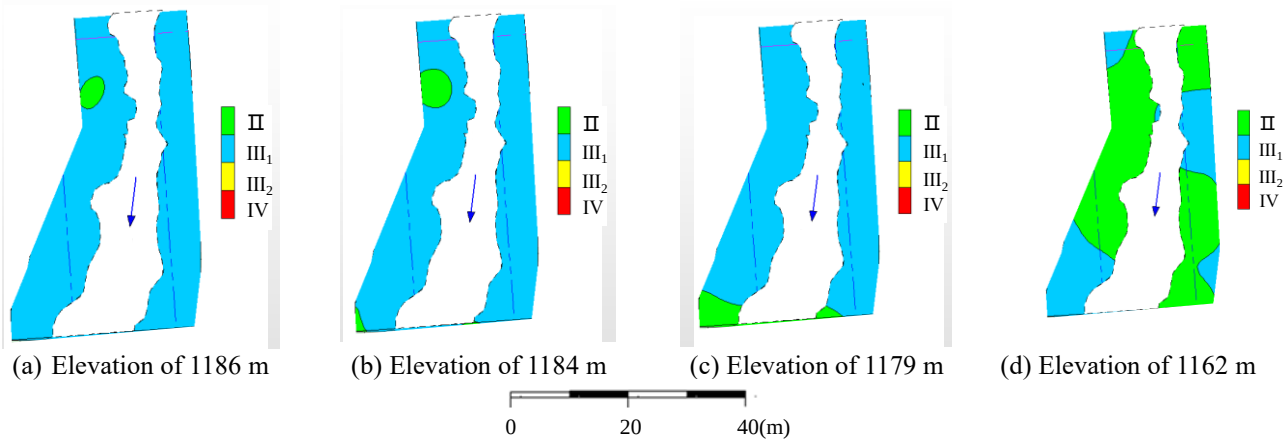

Fig. 18 Contour map of rock mass quality at different elevations

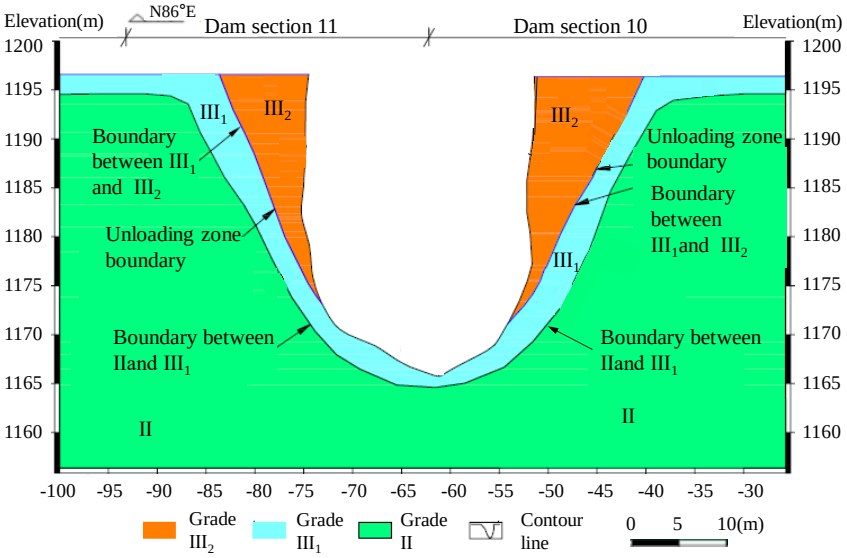

Fig. 19 Classification diagram of rock mass quality of 36.7 m downstream dam axis section

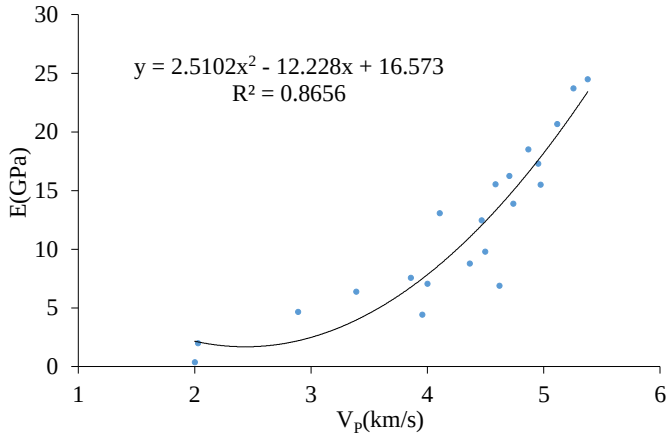

Fig. 20 Correlation curve between deformation modulus and P-wave velocity of dam foundation (E-deformation modulus (GPa); V_P - P-wave velocity (m/s))

unloading belt of the right wall is at the top part and decreases downward. No unloaded rock mass exists from 1173 m to the bottom. During the formation of the deep groove, the upper part of the rock mass unloaded towards the surface. Under the action of weathering and river flow patterns, the rock mass was further destroyed, causing the undisturbed rock mass to become exposed gradually and the unloading depth to deepen progressively. However, due to overburden filling, the unloading rock mass of the groove wall was not further exacerbated. The rock mass at the bottom was constantly subjected to mechanical erosion of water flow, which removed the loose rock mass. Under overburden load and gravity, the rock mass at the bottom unloaded upward slightly.

5. Rock mass classification and mechanical parameter

5.1 Rock mass quality

Longitudinally, in the exploration stage, it was speculated that the rock mass quality was good. In the early construction and excavation stage, dam sections 10 and 12 with grade III_1 rock mass were excavated first, thus inferring that the quality of the rock mass in dam section 11 was also good. In the middle stage of construction, the section 11 dam foundation was excavated to an elevation of 1197 m. The deep groove was gradually revealed. The minimum width of the deep groove was 6 m, the maximum width was close to 20 m, and the width in the dam foundation section was 11 ~ 16 m. In the early stage of deep groove disclosure, based on the research results of the dam foundation in the early stage, and the efficiency investigation, the quality of the deep groove rock mass was classified. The variation of the deep groove rock mass along the horizontal and vertical directions was obtained.

As shown in Table 3, the classification standard for the rock mass quality of the dam foundation was formulated according to the qualitative observation and test data obtained from boreholes and adits in the exploration stage.

The rock mass quality was well verified in the dam foundation excavation stage. The rock mass of grade II is slightly weathered and relatively intact, with high integrity coefficients and slight water permeability, which can be directly utilized. Grade III_1 is a slightly weathered to stage I of moderately weathered rock mass, with relatively poor to intact integrity, strong deformation resistance, and micro to weak water permeability, which can be fully utilized after engineering treatments. Grade III_2 is of stage II moderately weathered rock mass with poor rock mass integrity and weak water permeability, which can be partially used after engineering reinforcement. Grade IV is a stage II of moderately to strongly weathered rock mass, with tight intraformational partially faulted belts, developed structural planes, and weak ability to resist deformation. Grade V is a tough intercalation and extrusion fracture zone. The rock mass of the deep groove and the dam foundation are similar in composition, structure, weathering, and unloading. Therefore, the normal rock mass quality classification standard can be used for the deep groove. Taking DTH LSC-3 as an example, the division method of rock mass quality by the P-wave test is described as follows (Table 4).

According to the classification standard for rock mass quality of dam foundations, the rock mass quality of LSC-3 can be divided into three sections. Within the 0 ~ 2.0 m, the V_P values are mainly approximately 3000 m/s, with a slightly poor rock mass, and classified as grade IV. Within the 2 ~ 7.4 m range, rock mass quality improves, classified as grade III_2. Within the scope of 7.4 m to the bottom, the wave velocity is generally above 4200 m/s and classified as grade III_1.

Based on the structure, weathering, and unloading results, we speculated that the deep groove was not tectonic in origin. According to the preliminary data on the deep groove, the contour map of rock mass quality grade at different elevations below the foundation surface can be obtained. The contour maps of 1 m, 3 m, 8 m, and 25 m below the elevation of 1187 m are shown in Fig. 18. The grade of rock mass quality under the foundation surface ranges from grade III_1 to II. The quality of the rock mass is relatively uniform in the horizontal direction and increases gradually with increasing depth.

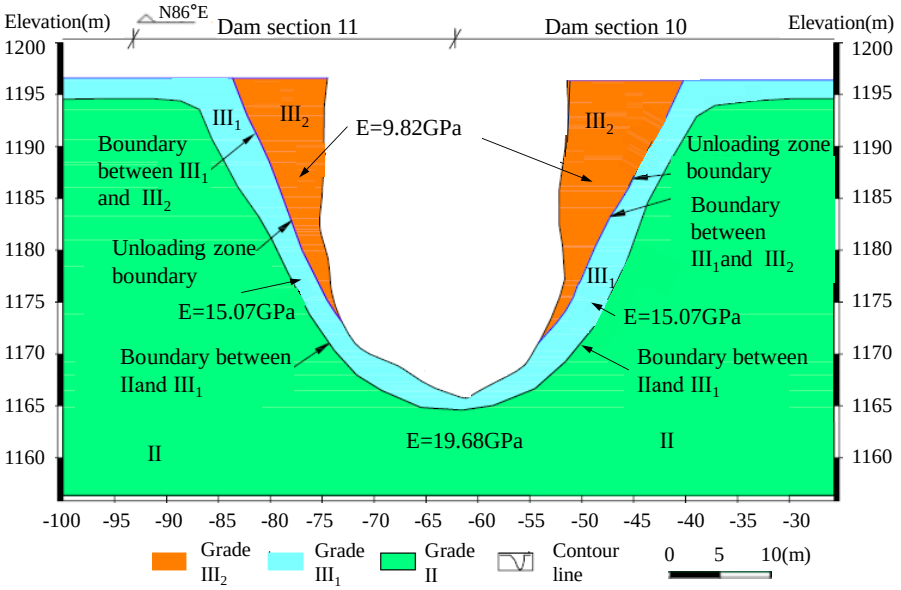

Fig. 21 Mechanical parameters corresponding to different rock mass grades of 36.7 m downstream dam axial section

With the exposure of the deep groove, the preliminary data of the rock mass quality were fed back. At the end of construction, the deep groove wall was utterly exposed, and the optimal rock mass quality data were obtained, which was consistent with the preliminary data. The transverse section of the 36.7 m downstream dam axis is taken as an example to analyze the characteristics of rock mass quality (Fig. 19).

As shown, the grade III_2 rock mass is relatively thick in the shallow part at 1197 ~ 1187 m elevations, gradually decreasing as depth increases. Due to blasting excavation, the surface rock mass quality of the groove wall at elevations of 1187 ~ 1170 m is grade III_2, which is slightly different from the contour map in Fig. 18. The rock mass quality at the bottom of the deep groove is grade III_1 within 5 m in the vertical direction. The quality of the rock mass gradually improves with increasing depth. Compared with normal rock mass at the same elevation, the quality of the deep groove rock mass decreases by 0.5 ~ 1 grade. The rock mass of the deep groove wall can be used as foundation after the loose rock mass excavated.

5.2 Mechanical parameters

The rock mass of stage II moderately weathered has poor integrity with low V_P. The rock mass of stage I moderately weathered and slightly weathered, is less disturbed, exhibiting higher mechanical properties and V_P in the in situ state. Therefore, it can be deduced that V_P corresponds to the mechanical parameters. In situ deformation tests cannot be performed in deep grooves but were carried out on other sections of the dam foundation in the exploration and construction stages. Based on these deformation tests and the corresponding V_P tests, the correlation between the deformation modulus and V_P was obtained, as shown in Fig. 20.

From the curve, the correlation between the deformation modulus and V_P is shown as follows

$$E = 2.5102V_P^2 - 12.228\ V_P + 16.573 \quad (1)$$

where V_P is the P-wave velocity, and E is the deformation modulus.

It can be seen from Fig. 20 that the deformation modulus has a good correlation with V_P. The correlation could be extended to research on the mechanical parameters of deep grooves. Based on the average value of the V_P of each rock mass grade, the deformation modulus of the deep groove rock mass can be deduced by the correlation formula. For example, the rock grades and mechanical parameters of 36.7 m downstream dam axis section is shown in Fig. 21.

Compared with the dam foundation, the deep groove rock mass unloaded to the free surface horizontally during formation. Secondary unloading and weathering occurred in the deep groove section, and the engineering characteristics changed substantially. In this section, the rock mass suddenly caved in for tens of meters, which destroyed the normal bedrock weathering zone and formed a new groove weathering zone.

Through the DTIEM, the preliminary engineering characteristics of the deep groove rock mass were obtained. The conclusion of the rock mass availability was drawn that the overlaying layer in the deep groove should be removed, and the quality of the deep groove rock mass was poor compared with that of the normal rock mass at the same elevation. The rock mass at the elevation of 1186 m was mainly grade III_1 and contained a small area of grade II. The quality increased with increasing depth in the vertical direction. The deformation modulus of grade III_1 was up to 15.07 GPa, which could be used as the dam foundation. Therefore, the rock mass of the groove wall at 1186 m elevation was taken as the foundation of an arch cross plate, which crossed the groove. Then, the dam body was poured on top of it. The deep groove was gradually revealed to recheck the preliminary data. Finally, the deep groove was

Table 5 Mechanical parameters of the numerical model materials

Material	Density (g/mm^3)	E (Mpa)	Poisson's ratio	c' (Mpa)	φ' (°)
Grade II	0.026	19680	0.2	2.3	52.43
Grade III$_1$	0.025	15070	0.25	1.18	49.24
Covering layer	0.01	3000	0.3	0.1	38
Arch cross-plate	0.024	28500	0.167		
Concrete dam	0.024	28500	0.167		
Rock mass of groove wall	0.025	13770	0.25	1.18	49.24

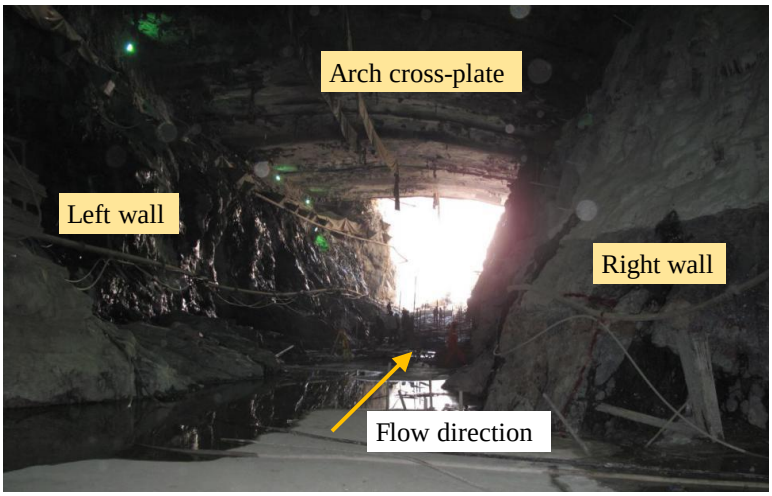

Fig. 22 Photo of arch cross-plate and deep groove internal morphology

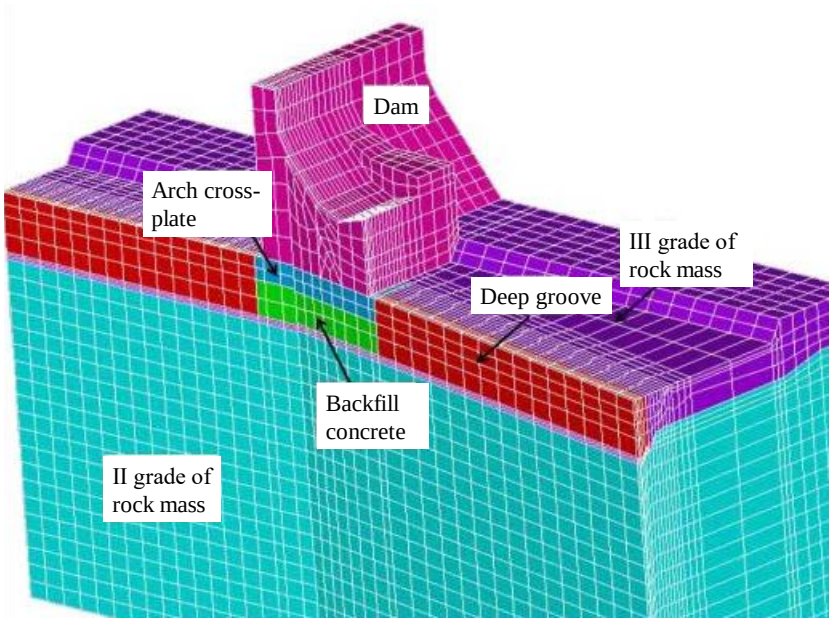

Fig. 23 Section diagram of 3D numerical model

backfilled by grouting. The final excavation results of the deep groove showed that the engineering geological characteristics were mostly the same as those of the preliminary data (Fig. 22). To ensure the safe operation of the hydropower station, monitoring devices were installed at crucial positions, such as at the gap between the arch plate and backfilled concrete.

6. Numerical simulation

To verify the reliability of the DTIEM applied to the deep groove, this paper used the finite element method to simulate the construction and water storage working conditions (Yalcin *et al*. 2016, Kim *et al.* 2020, Mohammad *et al*. 2021). The model includes the dam foundation, deep

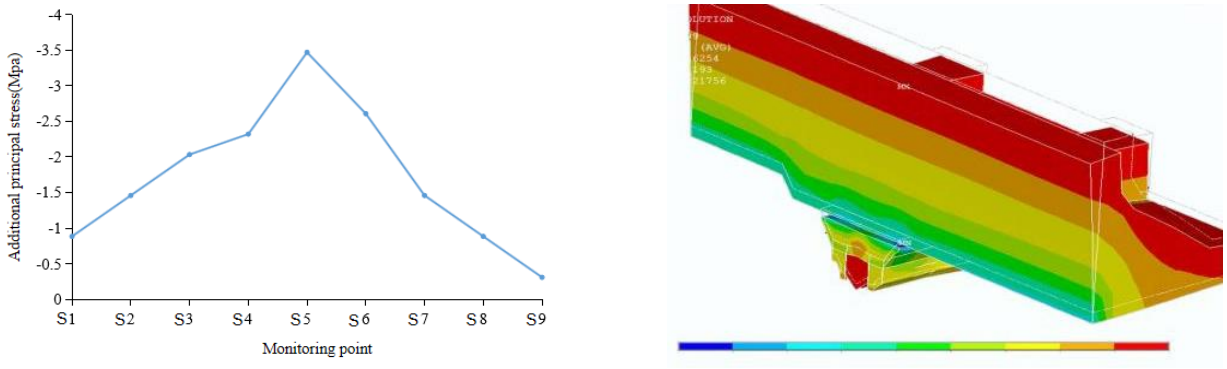

(a) Stress diagram (b) Stress cloud diagram

Fig. 24 Additional maximum principal trend diagram (a) and stress cloud diagram (b) of gravity dam, arch plate, and deep groove wall (MPa)

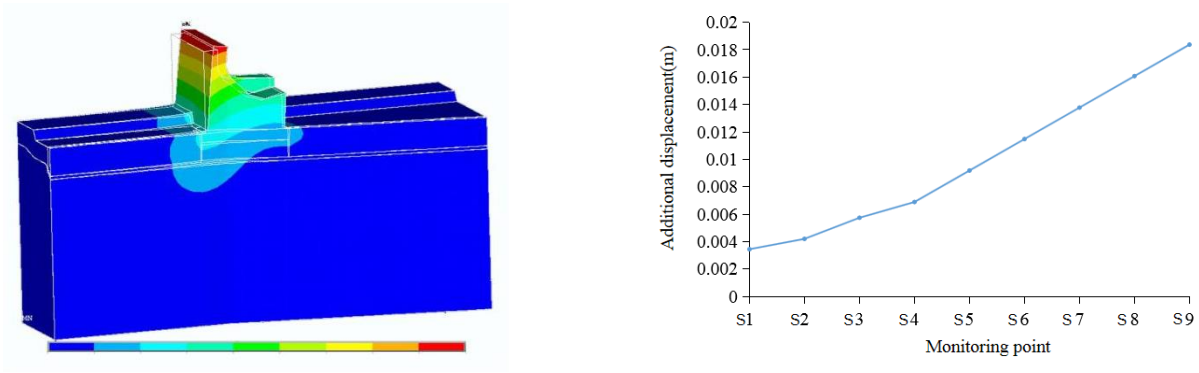

(a) Stress cloud diagram (b) Stress diagram

Fig. 25 Additional displacement cloud diagram (a) and trend diagram (b) of normal water level

groove, arch cross plate, and dam. The material parameters can be shown in Table 5. The model is 265 m in width (transverse river direction) and 540 m in length (river direction), with a total of 54,517 units (Fig. 23). The Drucker-Prager constitutive model was applied to define the material parameters. Gravity was applied to the model. The structural optimization grid technique was applied to divide the grid. The four surfaces and the bottom of the bedrock were designed as hinge bearings. Displacement control was used to ensure convergence. There were 7 stages in the model calculation. First, the deep groove was buried under the modern river valley. Second, the riverbed was excavated, and the deep groove was exposed. Third, an arch plate was poured across the deep groove. Fourth, the deep groove was excavated. Fifth, the gravity dam was poured on the cross plate. Sixth, concrete was backfilled in the deep groove. Seventh, the water behind the dam reached the normal reservoir level. The "death" and "life" commands of the unit in the software were used to simulate the excavation and backfilling of the deep grooves.

According to the preliminary data, the grade III_2 rock mass of the upper superficial groove wall should be excavated, and the grade III_1 rock mass at 1186 m elevation was taken as the foundation of the arch cross plate.

The dam body on the arch cross plate is 102.5 m high. After the dam body construction, the gravity dam loaded on the cross plate in the form of a uniformly distributed vertical load. The arch cross plate transferred the load to the deep groove wall. The stress and strain of the deep groove rock mass affected the stability of the whole upper structure. Monitoring points S1 and S2 were set at the bottom and middle part of the groove wall, S3 and S4 at the bottom and upper surface of the arch plate, and 5 monitoring points S5~S9 from the bottom to the top of the dam body. The trend of additional principal stresses at each monitoring point after the dam casting is shown in Fig. 24(a). The extra principal stress gradually increases from the bottom of the deep groove to the top of the arch plate, and progressively decreases from the bottom to the top of the dam body. The maximum value occurred at the bottom of the dam near the arch. From Fig. 24(b), it can be seen that the value of the additional principal stress at the bottom of the dam body forms a saddle-shaped distribution, which increases approximately 0 0.5 ~ 0.7 MPa compared with that in the other section of the dam due to the deep groove. There is no tensile stress zone in the plate or gravity dam.

During the operation of the hydropower station, the normal water level was at an elevation of 1298 m, and the gravity dam and foundation were subjected to water and uplift pressure. The simulation results of additional displacement and maximum principal stress are shown in Figs. 25 and 26.

As shown in Fig. 25, under water storage conditions, the additional maximum displacement is approximately 3 ~ 4

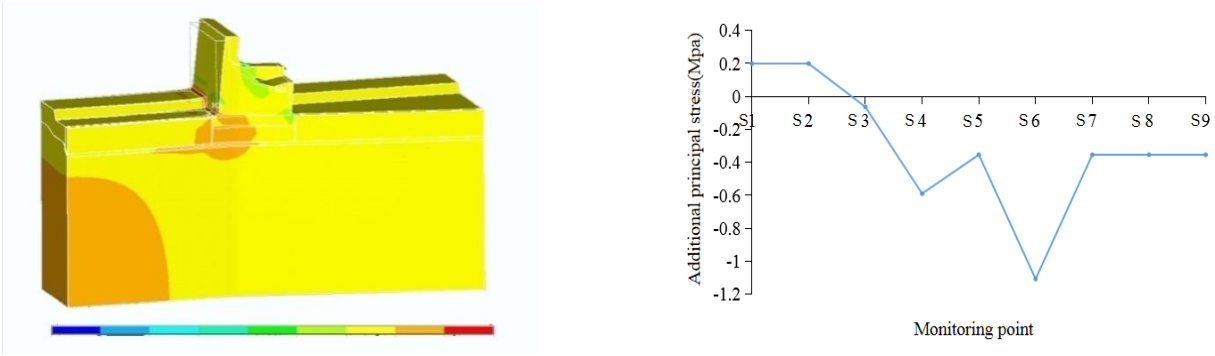

(a) Stress cloud diagram (b) Stress diagram

Fig. 26 Additional maximum principal stress cloud chart (a) and trend chart (b) of normal water level

Table 6 Structure classification scheme of dam foundation rock mass of Baihetan hydropower station (Nie 2007)

Structure type	*Kv*	*d* (cm)	V_P (m/s)
Monolithic block structure	0.8 ~ 1.0	> 100	>5500
Blocky structure	0.65 ~ 0.80	50 ~ 100	4850 ~ 5500
Blocky structure with low stiffness	0.55 ~ 0.75	> 50	4200 ~ 4850
Submassive structure	0.5 ~ 0.65	30 ~ 50	4200 ~ 4850
Mosaic structure	0.35 ~ 0.50	10 ~ 30	3500 ~ 4200
Loose block structure	0.35 ~ 0.50	30 ~ 100	3500 ~ 4200
Cataclastic structure	0.15 ~ 0.35	< 10	2300 ~ 3500
Loose structure	< 0.15		< 2300

Table 7 Quality classification of dam foundation rock mass of Jinanqiao hydropower station (Nie 2004)

Grade of rock mass quality		Structure type	V_P (m/s)
I		Massive structure	>5000
II		Blocky structure	4500 ~ 5500
III	III_a	Submassive-Mosaic structure	4000 ~ 5500
	III_b	Compact Mosaic structure	3500 ~ 4500
	III_c	In situ cataclastic structure	3000 ~ 4000
IV		Cataclastic structure	< 3000

mm for the deep groove, 6 ~ 8 mm for the arch plate, and 6 ~ 9 mm for the dam heel, which gradually increases as the elevation increases. The maximum value is approximately 20 mm at the top of the dam. The additional central stress cloud diagram (Fig. 26) reveals that after water storage, the bottom and middle of the deep groove are subjected to the action of additional tensile stress, which gradually transforms into pressure stress in the arch plate. The extra pressure stress at the lower part of the dam is the maximum and decreases with increasing elevation. According to the numerical simulation results, the stress and strain of the dam body are both within the safe range during the construction and operation period.

The field monitoring results after reservoir impounding are as follows: the gap opening between the arch cross plate and the backfill concrete is mostly less than 1 mm, the stress of the arch plate is less than 80 MPa, the displacement and deformation of the dam body are small, the seepage pressure of the dam foundation is slight, and there is no abnormal leakage (TAI 2014). In addition, the time limit of the entire construction project has not been affected too much. Combined with numerical simulation and monitoring results, it is fully proven that the rock mass engineering characteristics of deep groove obtained by the DTIEM are correct and reliable.

7. Discussion

Generally, if HCAGP is found in the construction stage, the safety and feasibility of the whole project would be questioned, and the entire project may even be suspended. Therefore, conducting a rapid investigation and evaluation of treatment plans is necessary. However, due to the limited construction conditions, the investigation and assessment of the HCAGP progressed slowly. For example, in July 2007, a large-scale weak extrusion zone was exposed after the excavation of the left dam foundation to the designed

Table 8 Quality classification and mechanical parameters of rock mass in Ertan hydropower station (Chengdu Engineering Co.Ltd.1990)

Grade of rock mass quality		Structure type	*d*(m)	*RQD*	V_P (m/s)
A		Massive structure	> 1	> 80	5800
B		Massive or blocky structure	0.6	75	5700
			0.6	75	5700
			0.6	75	5700
C	C-1	Blocky structure	0.5	70	5300
	C-2	Block Mosaic structure	0.4	60	5100
D	D-1	Mosaic structure	0.3	50	4400
	D-2	Mosaic cataclastic structure	0.3	40	4300
E	E-3	Cataclastic structure	0.25	30	3100

elevation of 222 m of the Xiangjiaba hydropower station. Due to the great depth, the small operating area, and the significant water seepage, exploration and construction took a lot of work. The treatment construction was not completed until February 2008, resulting in a severe delay in the construction period and significant losses. Nevertheless, under the same circumstance, the impact of the deep groove in this paper was minimized using the DTIEM.

The DTIEM used many DTH drill holes, with lower operational requirements, more convenient equipment, shorter construction periods, and higher work efficiency. Due to limited operating platforms and urgent construction schedules, DTH drilling was far better than traditional drilling, inclined wells, and other prospecting means. With the gradual investigation arrangement, DTH drilling was arranged in different directions step by step to minimize the amount of work instead of being arranged once and vertically only. Additionally, P-wave testing could be carried out in the drill holes instead of in situ testing, significantly minimizing the workload and improving work efficiency.

The reliability of V_P used in rock mass geological engineering research has been proven by many projects, as shown in Table 6 ~ 8. Therefore, V_P has been widely used in the DTIEM. According to the corresponding classification principle, the rock mass structure, weathering, unloading, and rock mass quality of the deep groove were obtained. In addition, the boundary points of each engineering characteristic were connected into surfaces by DTIEM to form a 3D boundary surface. The engineering characteristics at any location could be obtained by sectioning the 3D boundary surface.

For the study of the rock mass deformation modulus, some scholars have proposed using RQD (Zhang *et al.* 2004, Jiang *et al*. 2009), V_P (Song *et al*. 2011), RMR, Q (Mohammad *et al.* 2023), RMi (Yalcin *et al*. 2016), $E_{r\,dyn}$, $E_{r\,stat}$, $E_{m\,dyn}$ (Palmstrom *et al*. 2001) and other indicators for estimation. In addition, E_i, WD (E_i is the modulus of elasticity of the intact rock; WD is the weathering degree), SR, MR, FIS (Kayabasi *et al*. 2003), and RMQR (Aydan *et al.* 2014) have been proposed to assess the physical state of rock masses and used to estimate the geomechanical properties of rock masses.

For different lithologies, Alemda (2016) estimated the deformation modulus of stratified sedimentary rock masses using neural networks, fuzzy inference, and genetic programming. The relationship between wave velocity and physical-mechanical properties, such as the total and effective porosity, density, void ratio, water absorption, uniaxial compressive strength (UCS) and elastic modulus (E), of different lithologies were studied (Mohammad *et al*. 2019). These studies revealed correlations between the V_P and the mechanical parameters of the rock mass, which varied with different lithologies. It could be inferred that the classification criteria differed for different lithologies, which needed further study. In this study, we only obtained the correlation between V_P and deformation modulus but not that of other parameters. The classification criteria in this paper cannot be widely used for any other lithology, but the research method deserved popularization.

In short, through the numerical simulation of each stage and the monitoring results after the operation, it is concluded that the displacement and deformation of the dam are within a safe range, and there is no abnormal leakage, which verified that the method is practical and feasible. We believe that under certain conditions, this method can be applied to other similar projects. However, due to different engineering geological conditions, the formulas and standards may differ, but the general idea and process can be applied.

8. Conclusions

This paper proposed a dynamic-tracking investigation and evaluation method (DTIEM) for adverse geological phenomena revealed in the construction period, including a series of effective exploration techniques and evaluation methods, to obtain preliminary data. Accordingly, treatment and construction plans were made and continuously tracked and reviewed during construction. The process was applied to a deep groove in a hydropower station. Combined with the monitoring results and numerical simulation of deep groove, the following conclusions are obtained:

· The DTIEM is suitable for the particular investigation and evaluation of adverse geological phenomena highly

concealed in foundations. Firstly, the spatial distribution of hidden adverse geological phenomena can be quickly identified by gradually tracking small-diameter DTH holes, combined with exploration and geophysical prospecting. Then, with the help of the P-wave tests and the former investigation results, the initial engineering characteristics of rock mass can be obtained rapidly and accurately. Next, the treatment plan can be formulated, and the engineering characteristics of adverse geological phenomena are constantly tracked, improved, and refined during construction. The spatial distribution and the engineering Characteristics are tracked and refined step by step according to the order of "depth-width-cross section".

· Small-diameter holes such as down-the-hole holes that requires low construction conditions and has short working cycles are used in DTSM investigation, instead of conventional investigation methods such as drilling, shafts and adits.

· The DTIEM was applied to a deep groove of a hydropower station in China. According to the research results of the engineering characteristics of dam foundation rock mass obtained from the preliminary investigation, the wave velocity can accurately reflect the development of fissures and the engineering characteristics of the rock mass in this area. The research results showed that the rock mass quality of the top deep groove was grade III_2 with 9.82 GPa, the middle part was grade III_1 with 15.07 GPa, and the bottom part was grade II with 19.68 GPa. The quality of rock mass gradually increased with the increase of depth. Compared with normal rock mass at the same elevation, deep groove rock mass quality decreased by 0.5 ~ 1 of grade. Accordingly, after excavation, the rock mass at 1186 m elevation of the groove wall could be used as the foundation of the cross plate on which the dam body was poured.

· With the gradual excavation of the deep groove, the spatial shape and the engineering characteristics of rock mass were gradually revealed, which were basically consistent with the preliminary data. The numerical simulation showed that the maximum additional displacement was about 20 mm at the dam crest, 3~ 4 mm at the deep groove, 6 ~ 8 mm at the arch plate, and 6 ~ 9 mm at the dam heel. Through the numerical simulation of each stage and the monitoring results after the operation, it was concluded that the displacement and deformation of the dam were within a safe range, and there was no abnormal leakage. This outcome demonstrates that the DTIEM saves construction time to the greatest extent and has certain accuracy

Acknowledgments

This work described in this paper is fully funded by the Natural Science Research Project of Colleges and Universities in Anhui Province (grant No. 2022AH050963 and 2024AH050107); the Start Fund of Talent Introduction of Anhui Polytechnic University (grant No. 2023YQQ016).

References

Alemdag, S., Gurocak, Z., Cevik, A., Cabalar, A.F. and Gokceoglu, C. (2015), "Modeling deformation modulus of a stratified sedimentary rock mass using neural network, fuzzy inference and genetic programming", *Eng. Geol.*, **203**, 70-82. https://doi.org/10.1016/j.enggeo.2015.12.002.

Aydan, Ö., Ulusay, R. and Tokashiki, N. (2014), "A new rock mass quality rating system: Rock Mass Quality Rating (RMQR) and its application to the estimation of geomechanical characteristics of rock masses", *Rock Mech. Rock Eng.*, **47**(4), 1255-1276. https://doi.org/10.1007/s00603-013-0462-z.

Bednarek, U. and Majcherczyk, T. (2020), "An analysis of rock mass characteristics which influence the choice of support". *Geomech. Eng.*, **21**(4), 371-377. https://doi.org/10.12989/gae.2020.21.4.371.

Cai M., Kaiser P.K., Uno H., Tasaka Y. and Minami M. (2004), "Estimation of rock mass deformation modulus and strength of jointed hard rock masses using the GSI system", *Int. J. Rock Mech. Min.*, **41**(1), 3-19. https://doi.org/10.1016/S1365-1609(03)00025-X.

Chen, Y.L., Han, K. and Chen, Y.X. (2015), "Application of controlled source audio magnetotelluric method in karst collapse investigation", *Prog. Geophys.*, **30**(6), 2616-2622. https://doi.org/10.CNKI:SUN:DQWJ.0.2015-06-021.

Feng, Y.D. and Yang, J. (2009), "Application of integrated geophysical prospecting in the exploration of deep overburden in riverbed", *Chin. J. Eng. Geophys.*, **6**(2), 208-211. https://doi.org/10.CNKI:SUN:GCDQ.0.2009-02-017.

Hasan, M., Shang, Y., Yi, X., Shao, P. and Meng, H. (2023), "Determination of rock quality designation (RQD) using a novel geophysical approach: a case study", *B. Eng. Geol. Environ.*, 82. https://doi.org/10.1007/s10064-023-03113-7.

Jiang, X.W., Wan, L., Wang, X.S., Wu, X. and Cheng, H.H. (2009), "Estimation of depth-dependent hydraulic conductivity and deformation modulus using RQD", *Rock Soil Mech.*, **30**(10), 3163-3167. https://doi.org/10.1016/S1874-8651(10)60073-7.

Kahraman, S. and Yeken, T. (2008), "Determination of physical properties of carbonate rocks from P-wave velocity", *B. Eng. Geol. Environ.*, **67**, 277-281.

Kim, J.W., Chong, S.H., Cho, G.C. and Song, K.I. (2020), "Preliminary numerical study on long-wavelength wave propagation in a jointed rock mass", *Geomech. Eng.*, **21**(3), 227-236. https://doi.org/10.12989/gae.2020.21.3.227.

Kim, J.S., Kim, G.Y., Baik, M.H. and et al. (2019), "A new approach for quantitative damage assessment of in situ rock mass by acoustic emission", *Geomech. Eng.*, **18**(1), 11-20. https://doi.org/10.12989/gae.2019.18.1.011.

Kim, J.W., Chong, S.H. and Cho, G.C. (2022), "Probabilistic Q-system for rock classification considering shear wave propagation in jointed rock mass", *Geomech. Eng.*, **30**(5), 449-460. https://doi.org/10.12989/gae.2022.30.5.449.

Liu, S.H. (2016), "Sludging of soft interlayer in Bapanxia dam foundation and dam safety analysis", *Northwest Hydropower*, (4), 8-14. https://doi.org/10.3969/j.issn.1006-2610.2016.04.003.

Lu, X.Y., Gao, P.F., Xiao, G.Q., *et al.* (1996), "Quality acceptance criteria for rock mass on foundation surface of Three Gorges Dam", *Chin. J. Rock Mech. Eng.*, **15**(10), 599-604. https://doi.org/10.ConferenceArticle/5aa742e2c095d72220fb99bf.

Palmstrom, A. and Singh, R. (2001), "The deformation modulus of rock masses comparisons between in situ tests and indirect estimates", *Tunn. Undergr. Sp. Tech.*, **16**(2), 115-131. https://doi.org/10.1016/S0886-7798(01)00038-4.

Pappalardo, G. (2015), "Correlation between P-wave velocity and physical–mechanical properties of intensely jointed dolostones,

peloritani mounts, NE sicily", *Rock Mech. Rock Eng*., **48**(4), 1711-1721. https://doi.org/10.1007/s00603-014-0607-8.

Que, X., Zhu, Z., He, Y., Niu, Z. and Huang, H. (2023), "Strength and deformation characteristics of irregular columnar jointed rock mass: A combined experimental and theoretical study", *J. Rock Mech. Geotech*., **15**(2), 429-441. https://doi.org/10.1016/j.jrmge.2022.03.007.

Rezaei, M. and Davoodi, P.K. (2019), "Determining the relationship between shear wave velocity and physicomechanical properties of rocks", *Int. J. Min. Geo-Eng*., **55**(1), 65-72. https://doi.org/10.22059/IJMGE.2019.275851.594782.

Rezaei, M. and Habibi, H. (2023), "Designing of the Beheshtabad water transmission tunnel based on the hybrid empirical method", *Struct. Eng. Mech*., **86**(5), 621-633. https://doi.org/10.12989/sem.2023.86.5.621.

Rezaei, M. and Rajabi, M. (2021), "Assessment of plastic zones surrounding the power station cavern using numerical, fuzzy and statistical models", *Eng. Comput-Germany*, **37**, 1499-1518. https://doi.org/10.1007/s00366-019-00900-3.

Sarkar, K., Vishal, V. and Singh, T.N. (2012), "An empirical correlation of index geomechanical parameters with the compressional wave velocity", *Geotech. Geol. Eng*., **30**, 469-479.

Song, Y.H., Ju, G.H. and Sun, M. (2011), "Relationship between wave velocity and deformation modulus of rock masses", *Rock Soil Mech*., **32**(5), 1507-1513. https://doi.org/10.1631/jzus.B1000185.

Yalcin, E., Gurocak, Z., Ghabchi, R. and Zaman, M. (2016), "Numerical analysis for a realistic support design: Case study of the Komurhan tunnel in Eastern Turkey", *Int. J. Geomech*., **16**(3), https://doi.org/10.1061/(ASCE)GM.1943-5622.0000564.

Yin, M.L., Zhang, J.X., Jiang, Y.S., Jiang, H. and Shang, X.X. (2021), "Study on structural plane category modification of rock mass integrity coefficient characterized by rock mass volume joint number", *Rock Soil Mech*., **51**(11), 7. https://doi.org/10.16285/j.rsm.2020.0663.

Yu, S. (2007), "Analysis of deep anti-sliding stability of dam foundation in two dam sections of Xiangjiaba Hydropower Station", Ph.D. Dissertation, China University of Geosciences, Beijing.

Zhang, Y. (2010), "Advanced information analysis and optimization research on foundation rock mass of high concrete gravity dam", Ph.D. thesis, College of environment & civil engineering, Chengdu university of technology, Chengdu, China.

Appendix

The following symbols are used in this paper:

K_B = velocity ratio
K_V = integrity index
q = lugeonvalue
$E0$ = = modulus of deformation
V_P = P-wave velocity
f' = coefficient of shear friction
φ' = angle of internal friction
c' = shear cohesion
E_i = modulus of elasticity of the intact rock
WD = weathering degree
SR = simple regression equation
MR = multiple regression equation
FIS = fuzzy inference system
E_m = modulus of deformation of rock mass (in GPa)
RMR = rock mass rating system (Bieniawski 1973)
Q = Q system (Barton *et al.* 1974)
σ_c = uniaxial compressive strength (in MPa) of intact rock measured on 50mm diameter samples
RMi = rock mass index (Hoek and Brown 1998)
GSI = geological strength index (Hoek and Brown 1998)
$E_{r\,dyn}$ = dynamic elasticity modulus of intact rock
$E_{r\,stat}$ = static elasticity modulus of intact rock
$E_{m\,dyn}$ = dynamic in situ deformation modulus
RMQR = rock mass quality rating